VISCOELASTIC BEHAVIOR OF ERYTHROCYTE MEMBRANE

AYDIN TÖZEREN, RICHARD SKALAK, KUO-LI PAUL SUNG, AND SHU CHIEN
Bioengineering Institute and Department of Physiology, College of Physicians and Surgeons, Columbia University, New York, New York 10032

ABSTRACT A nonlinear viscoelastic relation is developed to describe the viscoelastic properties of erythrocyte membrane. This constitutive equation is used in the analysis of the time-dependent aspiration of an erythrocyte membrane into a micropipette. Equations governing this motion are reduced to a nonlinear integral equation of the Volterra type. A numerical procedure based on a finite difference scheme is used to solve the integral equation and to match the experimental data. The data, aspiration length vs. time, is used to determine the relaxation function at each time step. The inverse problem of obtaining the time dependence of the aspiration length from a given relaxation function is also solved. Analytical results obtained are applied to the experimental data of Chien et al. 1978. *Biophys. J.* 24:463–487. A relaxation function similar to that of a four-parameter solid with a shear-thinning viscous term is proposed.

1. INTRODUCTION

Membrane viscoelasticity plays an important role in various cell deformation processes such as cell division, response of endothelial cells to stress, and blood rheology. Viscoelastic properties of the erythrocyte membrane are of particular interest for the study of blood in health and disease (Chien, 1975; Skalak, 1976; Schmid-Schönbein, 1976). It is well established that the elastic modulus of the erythrocyte membrane under isotropic tension is several orders of magnitude higher than the shear modulus measured at constant area. This behavior has been incorporated into a single strain energy function consisting of two terms (Skalak et al., 1973; Evans, 1973; Evans and Skalak, 1979); one term gives the low elastic modulus observed when the membrane is deformed at constant area and the other represents the high elastic modulus encountered when the area is increased.

Viscoelastic properties of the erythrocyte membrane have been investigated with several rapid-transient experiments (Evans and Hochmuth, 1976; Chien et al., 1978). The former considered recovery after release of an elongated erythrocyte, and the latter used a micropipette to perform both loading and recovery experiments. These experimental results were analyzed using a two-dimensional Kelvin model proposed by Evans and Hochmuth (1976). The results of Chien et al. (1978) showed that the deformation of a cell in a pipette following a step load consisted of two phases: the initial phase was characterized by large and rapid deformations and low membrane viscosity; the final one exhibited a high membrane viscosity and small deformation. Moreover, the experiments of Chien et al. (1978) suggest that the rapid phase of deformation has a shear-thinning behavior. It is the aim of the present paper to model this shear-thinning process. For this purpose, a constitutive relation in the form of an integral equation is introduced.

Coleman and Noll (1961) have developed a theory for finite deformations of a viscoelastic solid using the concept of fading memory. Another formulation given by Pipkin and Rogers (1968) has been applied to the axially symmetric deformation of viscoelastic membranes with rubberlike elasticity (Wineman, 1972; Wineman, 1978). Single integral relations have also been used by Fung (1972) and Skalak (1976) to describe the time-dependent behavior of biological soft tissues.

In the present treatment of the micropipette problem, separate solutions are first obtained for the portions of the membrane inside and outside of the pipette. It is then shown that the membrane relaxation function and the time history of cell deformation in the pipette can be related in a single nonlinear integral equation.

A numerical procedure is developed to calculate the relaxation function for a given time history of deformation and recovery in the pipette. The same computational scheme is applied to calculate the cell deformation as a function of time for a given relaxation function.

Analysis of micropipette data shows that the relaxation function strongly depends on the magnitude of the applied pressure difference. This shear-thinning behavior of erythrocyte membrane was previously noted by Chien et al. (1978), but not incorporated into a model. In the present model the two time constants and the shear-thining behavior observed in the experiments are incorporated. The theoretical model is shown to describe the time history of erythrocyte membrane deformation satisfactorily over the entire range of aspiration studied in the experiments.

2. THE CONSTITUTIVE EQUATION

A general viscoelastic constitutive equation for the erythrocyte membrane may be written in terms of principal strains and stresses. This implies no loss of generality, assuming the membrane is isotropic in its own plane. Let any deformation of the membrane be described by initial positions X_1, X_2 and current positions Y_1, Y_2 in a coordinate system tangent to the local principal directions. Extension ratios λ_1 and λ_2 are defined as

$$\lambda_1 = (dY_1/dX_1), \lambda_2 = (dY_2/dX_2). \quad (1)$$

The surface area of the membrane is assumed to remain constant. This requires

$$\lambda_1\lambda_2 = 1. \quad (2)$$

The membrane strain energy function for a constant surface area may be expressed in terms of the strain invariant I_1 (Skalak et al., 1973):

$$I_1 = \lambda_1^2 + \lambda_2^2 - 2. \quad (3)$$

The steady-state elastic behavior of the cell membrane (Evans, 1973) is conveniently described by a stress-strain relation of the form

$$T_1 = T_0 + \mu(\lambda_1^2 - 1), T_2 = T_0 + \mu(\lambda_2^2 - 1) \quad (4)$$

where μ is the shear modulus of elasticity and T_0 is an isotropic stress that arises due to the constant area stipulation. Eq. 4 describes the membrane behavior in static-pipette experiments with an average value for μ of 4.2×10^{-3} dyn/cm (Chien et al., 1978).

Membrane tensions T_1 and T_2 are related to the Piola-Kirchoff stresses S_1 and S_2 by (Skalak et al., 1973)

$$T_1 = (\lambda_1/\lambda_2)S_1, T_2 = (\lambda_2/\lambda_1)S_2. \quad (5)$$

In the following text a description of nonlinear viscoelastic behavior of a membrane will be developed using an integral formulation. Let $\tilde{S}_1$ and $\tilde{S}_2$ represent the Piola-Kirchoff stress resultants excluding the isotropic tension T_0; i.e.,

$$\tilde{S}_1 = (\lambda_2/\lambda_1)(T_1 - T_0), \tilde{S}_2 = (\lambda_1/\lambda_2)(T_2 - T_0). \quad (6)$$

For a unit step-strain input, $\tilde{S}_1$ and $\tilde{S}_2$ are assumed to be of the form

$$\tilde{S}_1 = \mu G(t, I_1, \dot{I}_1)(1 - \lambda_2^2),$$
$$\tilde{S}_2 = \mu G(t, I_1, \dot{I}_1)(1 - \lambda_1^2) \quad (7)$$

where G is a relaxation function, t is the time measured from the instant of application of the step in strain, and $\dot{I}_1$ denotes the material time derivative of I_1. The stress produced by any continuous strain history can be obtained by integration with Eq. 7:

$$T_1 = T_0 + \mu\lambda_1^2 \int_0^t G(t - s, I_1, \dot{I}_1) \frac{d}{ds}[1 - \lambda_2^2(s)]ds$$

$$T_2 = T_0 + \mu\lambda_2^2 \int_0^t G(t - s, \dot{I}_1, I_1) \frac{d}{ds}[1 - \lambda_1^2(s)]ds \quad (8)$$

where $\lambda_1(s), \lambda_2(s)$ are the specified strain history.

Single-integral representation for finite viscoelastic deformation was introduced by Pipkin and Rogers (1968). This is the first term of a series based on the response of the material to a series of step-strain inputs. The relaxation function G is usually assumed to be dependent only on elapsed time $(t - s)$ for soft biological materials (Fung, 1972).

The membrane will have instantaneous elastic response if G is finite for all times $(t - s) \geq 0$. To incorporate viscous behavior, G is written as the sum

$$G = G^*(0)\tau(t, I_1, \dot{I}_1)\delta(t) + G^*(t) \quad (9)$$

where τ is a function having units of time and plays the role of a variable time constant; $\delta(t)$ is the Dirac delta function. The first term of Eq. 9 provides a viscous type of response. The second term, $G^*(t)$, incorporates viscoelasticity and is assumed to be independent of strain.

Eqs. 8 and 9 reduce to the constitutive equation (Kelvin material) proposed by Evans and Hochmuth (1976) if $G^*(t)$ is equal to unity and τ is a constant. On the other hand, the membrane will show instantaneous elastic response only if τ is identically equal to zero. In that case, the instantaneous elastic response and the long-term elastic behavior are described by the same stress-strain relation but with different values of the elastic coefficient.

The deviatoric part $(T_1 - T_2)$ of membrane tensions may be written in the more convenient form

$$T_1 - T_2 = \mu\Big(4G^*(0)\tau(\dot{\lambda}_1/\lambda_1) + G^*(0)(\lambda_1^2 - \lambda_2^2) + \int_0^t C^*(t - s)\{\lambda_1^2(t)[1 - \lambda_1^{-2}(s)] - \lambda_1^{-2}(t)[1 - \lambda_1^2(s)]\}ds\Big) \quad (10)$$

where $\dot{\lambda}_1$ is the time derivative of λ_1, and C^* is the derivative of G^* with respect to $(t - s)$ $[C^*(t - s) = dG^*(t - s, I_1, \dot{I}_1)/d(t - s)]$.

In the case of a uniaxial tension test in which the stretch ratio λ_1 and T_1, T_2 are measured as functions of time, Eq. 10 can be used to determine the relaxation function G. The micropipette experiments are not simple uniaxial tension tests; however, as discussed in the next section, they can be used to determine the relaxation function.

3. ANALYSIS OF THE MICROPIPETTE EXPERIMENT

The analysis of erythrocyte aspiration into a micropipette will be based on an approximation of the cell membrane as an infinite plane that is aspirated into a tube of radius R_p. This model was introduced by Evans (1973) and was recently used by Chien et al. (1978). Let R', ϕ', Z' be cylindrical coordinates and set $R = R'/R_p$ and $Z = Z'/R_p$. Further, let the dimensionless coordinates (R_0, ϕ_0, Z_0) and (R, ϕ, Z) denote the initial and deformed coordinates of the same material point of the membrane (Fig. 1). A dimensionless variable A is defined by letting $\pi R_p^2 A$ denote the membrane surface area of the portion of the cell aspirated into the pipette. In the experiments, aspiration length D_p is measured as a function of time, t. The relation between (D_p/R_p) and the dimensionless aspiration area A is usually based on a spherical cap model. A better approximation is derived in the Appendix.

The membrane deformation in the micropipette experiment is assumed to occur at constant surface area. Thus the time-dependent deformation of the planar portion of the membrane outside the pipette is described by $R = R(R_0, t)$:

$$R^2 = R_0^2 - A(t) + 1, R \geq 1. \tag{11}$$

The extension ratio λ_1 and the rate of strain V_{11} in the radial direction can be expressed as follows for the region outside the pipette $(R \geq 1)$:

$$\lambda_1^2 = (dR/dR_0)^2 = (R^2 + A(t) - 1)/R^2 \tag{12}$$

$$V_{11} = (\mathring{\lambda}_1/\lambda_1) = \mathring{A}(t)/2R^2. \tag{13}$$

With Eq. 11, the history of the stretch ratio λ_1 can be described as a function of previous time s by

$$\lambda_1^2(s) = [R^2(t) + A(t) - 1]/ \cdot [R^2(t) + A(t) - A(s)]\ 0 < s < t \tag{14}$$

where $\lambda_1(s)$ is the stretch ratio history of the material which occupies position R at time t. The value $\lambda_1(s)$ occurs at time s. Eqs. 12–14 completely describe the time history of deformation for $R > 1$ as a known function of position (R), the aspirated surface area history, $A = A(t)$, and the previous time, (s).

Equations of equilibrium are now considered to relate the relaxation function of the membrane to the deformation. The equilibrium of the membrane inside the pipette requires that

$$(2T_p/\mu) = (R_p \Delta P^*/\mu)\sin(\theta_0) \tag{15}$$

where θ is the angle that the normal to the meridian makes with the axis of symmetry and θ_0 is the value of this angle at the tip of the pipette. T_p is the meridianal tension at the tip of the pipette and ΔP^* can be related to the total pressure difference across the membrane. The pressure ΔP^* can be related to the total pressure across the pipette by the following equation:

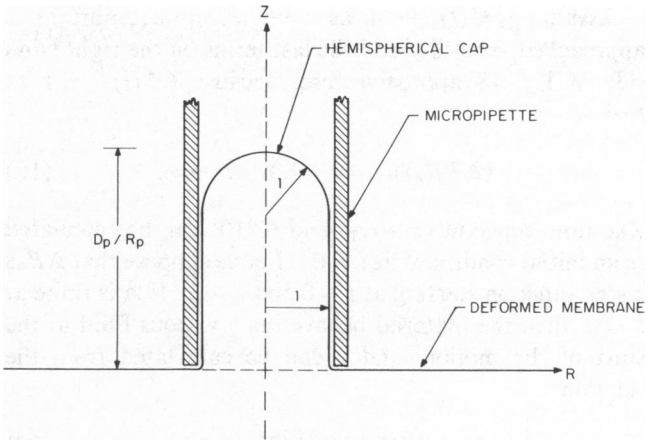

FIGURE 1 Schematic diagram of membrane aspiration.

$$\Delta P^* = h(t)\Delta P - 2\tau_f \mathring{A} G^*(0)\mu/R_p \tag{16}$$

where $h(t)\Delta P$ is the applied pressure difference. The dimensionless function $h(t)$ is approximately a step function and τ_f is a time constant that is introduced to account for the dissipation due to the fluids inside and outside the cell. The viscosity of the fluids makes $\Delta P^* < \Delta p$.

The equilibrium equations of the flat part of the membrane (see Chien et al., 1978) require that

$$T_p = \int_1^\infty (T_1 - T_2)\, dR/R \tag{17}$$

where T_1 and T_2 are the radial and circumferential tensions. In writing Eq. 17, the membrane is assumed to slide freely over the tip of the pipette. The difference in principal tensions, $(T_1 - T_2)$, can be expressed in terms of the history of the stretch ratio λ_1 by Eq. 10. Eq. 17 then involves double integration with respect to R and s. However, integration with respect to R can be performed analytically by recognizing that R and s are independent variables. After integrating Eq. 17 with respect to R and combining the result with Eq. 14 and 15, one obtains

$$h(t)(R_p \Delta P/\mu)/\sin\theta_0 = 2(\tau + \tau_f)G^*(0)\mathring{A} + G^*(t)F[A(t)] - \int_0^t C^*(t - s)F[A(t) - A(s) + 1]\, ds \tag{18}$$

where $F(A) = \ln A + A - 1$.

Eq. 18 is a nonlinear, integral relation of the Volterra type governing the deformation phase of the pipette aspiration. It may be used to calculate A as a function of t for a given relaxation function G, or vice versa. The numerical solution of Eq. 18 will be discussed in section 4. Some general features of the solution are discussed below.

Assuming $H(t) \rightarrow 1$ as $t \rightarrow \infty$, an equilibrium is approached. The first and the last terms on the right hand side of Eq. 18 approach zero, because $G^*(t) \rightarrow 1$ as $t \rightarrow \infty$

$$(\Delta P R_p/\mu) = F(A_p), \quad t \rightarrow \infty. \tag{19}$$

The time constant $(\tau + \tau_f)$ and $G^*(0)$ can be calculated from initial conditions at $t = 0^+$. Let us suppose that ΔP is a step function starting at $t = 0$ and $\tau_f = 0$. If $\mathring{A}$ is finite at $t = 0$, then the material behaves as a viscous fluid at the start of the motion, and τ can be calculated from the relation

$$\tau = F(A_p)/(2\mathring{A}(0)\sin\theta_0). \tag{20}$$

On the other hand, if the material has instantaneous elastic response, $G^*(0)$ is determined by the nonlinear equation

$$F(A_p) = G^*(0)F(A_i)\sin\theta_0 \tag{21}$$

where A_i is the value of A taken instantaneously at $t = 0^+$ after application of the pressure difference ΔP.

In the pipette experiment, cell membrane is studied by suddenly removing the aspiration pressure. In analyzing the recovery phase, the previous deformation history must be taken into account. Eq. 14 relates the deformation at time s to the deformation at time t and it is valid for the relaxation phase if $R(s)$ lies in the planar portion of the membrane. On the other hand, material points occupying position R at time t may still be inside the pipette at time s. For such points

$$\lambda_1^2(s) = R^2 + A(t) - 1,$$
$$1 < R^2 < 1 - A(t) + A(s). \tag{22}$$

For the analysis of the recovery phase let $t = 0$ denote the time of release and let $t = -t_0$ be the starting time of the loading phase. The integral equation governing the recovery phase can be obtained, by integrating the equilibrium equation (17) analytically with respect to R. The tension T_p at the tip of the pipette in this case is set equal to zero. The result is

$$2(\tau + \tau_f)G^*(0)\mathring{A} + \int_{t^*}^{t} C^*(t-s)F[A(s) - A(t) + 1]\,ds - \int_{-t_0}^{t^*} C^*(t-s)F[A(t) - A(s) + 1]\,ds + G^*(t + t_0)F[A(t)] = 0, \tag{23}$$

where t^* is such that $A(t) > A(s)$ if $s < t^*$. The first two terms in Eq. 23 have negative values while the last two terms have positive values during the recovery phase. The last integral in Eq. 23 approaches zero as the duration of the loading phase, t_0, becomes sufficiently large. This limiting case is governed by the simpler equation:

$$2(\tau + \tau_f)\mathring{A}G^*(0) + \int_0^t C^*(t-s) \cdot F[A(s) - A(t) + 1]\,ds + [1 - G^*(t)] \cdot F[A_p - A(t) + 1] + F[A(t)] = 0 \tag{24}$$

where A_p is the maximum value reached during the deformation phase. Eqs. 23 and 24 show the dependence of the relaxation phase on the duration of the deformation phase. The sooner the relaxation phase starts the larger will be the last two terms in Eq. 24. Hence the membrane will relax faster if the deformation phase is shorter as observed in experiments by Chien et al. (1978).

Integral Eqs. 18 and 23 involve the dimensionless surface area A as a time-dependent function. However, in actual experiments only the aspiration length D_p is measured as a function of time. In previous studies, D_p and A were related by assuming the cap inside the pipette was part of a sphere. The exact elastic membrane solution for the cap inside the pipette is considered in the appendix to obtain a more accurate relation among D_p, R_p, and A.

The profiles of several membrane caps obtained by integration of membrane equations are shown in Fig. 2 for various values of $(\Delta P R_p/\mu)$. The cap becomes spherical in the limit as $(\Delta P R_p/\mu)$ approaches infinity or zero.

The aspiration length D_p/R_p is shown as a function of A and of $(\Delta P R_p/\mu)$ in Figs. 3 and 4, respectively. The relations given by the spherical cap model (Chien et al., 1978) are also shown for comparison. It is apparent that for a given value of the parameter $(\Delta P R_p/\mu)$ the spherical-cap assumption predicts slightly smaller values for D_p and A than the exact membrane solution. This also holds for the spheroidal cap model of Evans (1973).

The value of the circumferential radius of curvature ($R_2' = R_p R_2$, see Appendix) at the tip of the pipette is important in estimating the membrane tension T_p at that point. The curvature R_2 at the tip of the pipette computed

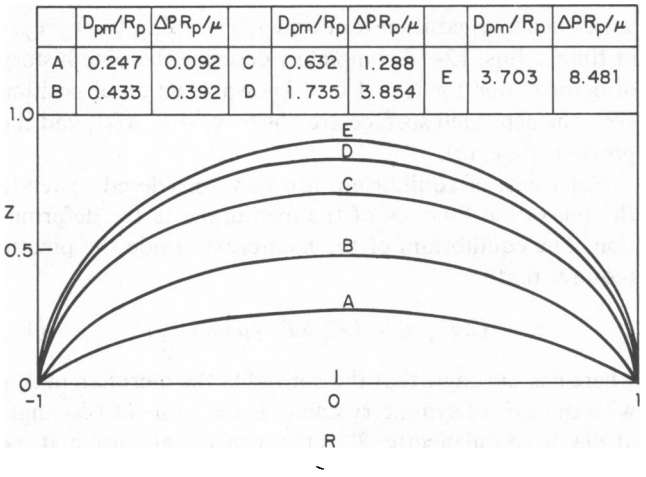

FIGURE 2 Profiles of the membrane cap as a function of dimensionless aspiration length.

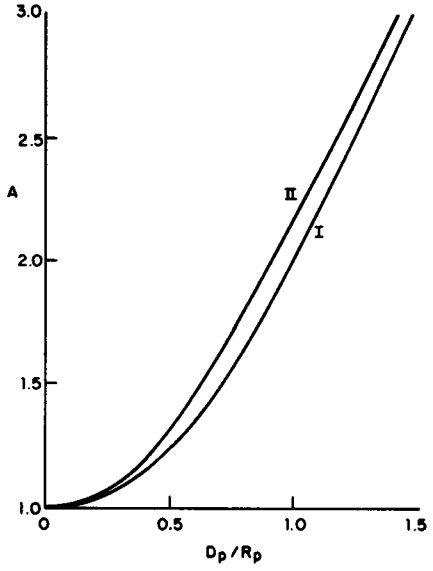

FIGURE 3 Dimensionless surface area A as a function of (D_p/R_p) obtained by present theory in comparison with results of spherical cap model. I, spherical cap model; II, exact membrane solution.

from the exact solution is compared in Fig. 5 with the corresponding curvature from the spherical cap model. The tension T_p of the spherical cap is larger than that obtained by the exact solution in proportion to these curvatures. The bending resistance of the membrane may play an important role when the value for maximum aspiration (D_{pm}/R_p) is sufficiently small. However, if the maximum aspiration (D_{pm}/R_p) is > 1.0, the membrane tension T_1 will still predominate. Hence, in the following analysis the exact membrane solution derived in the Appendix will be used.

4. NUMERICAL COMPUTATIONS AND THE DISCUSSION OF THE VISCOELASTIC INTEGRAL EQUATION

It was shown by Chien et al. (1978) that the experimental aspiration length history during the loading phase can be

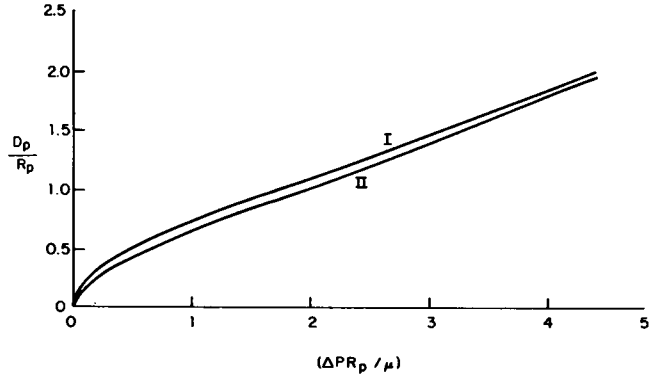

FIGURE 4 Steady-state deformation (D_{pm}/R_p) as a function of dimensionless membrane tension $(\Delta P\ R_p/\mu)$ obtained by exact membrane analysis, showing good agreements with spherical cap model. I, spherical cap model; II, exact membrane solution.

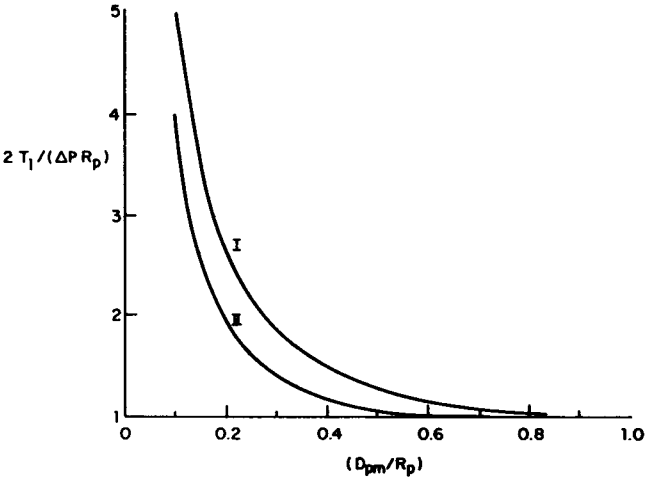

FIGURE 5 Tension T_p at the tip of the pipette as a function of (D_p/R_p): I, spherical cap model; II, exact membrane solution.

approximated by two exponential functions (Fig. 6) of the form

$$\frac{D_p}{R_p} = \frac{D'_{pm}}{R_p}(1 - e^{-t/\beta_1}) + \left(\frac{D_{pm}}{R_p} - \frac{D'_{pm}}{R_p}\right)(1 - e^{-t/\beta_2}) \quad (25)$$

where D_{pm} is the maximum aspiration length achieved in that particular experiment, D'_{pm} is the apparent steady-state deformation attained in the first rapid phase, and β_1 and β_2 are time constants. The experiments show that $\beta_1 \ll \beta_2$ and $(D_{pm} - D'_{pm}) \ll D_{pm}$. The value β_1 is shown to decrease with increasing $(\Delta P R_p/\mu)$ but β_2 is not correlated with the degree of deformation. The function $A(t)$ is determined from the experimentally measured values for

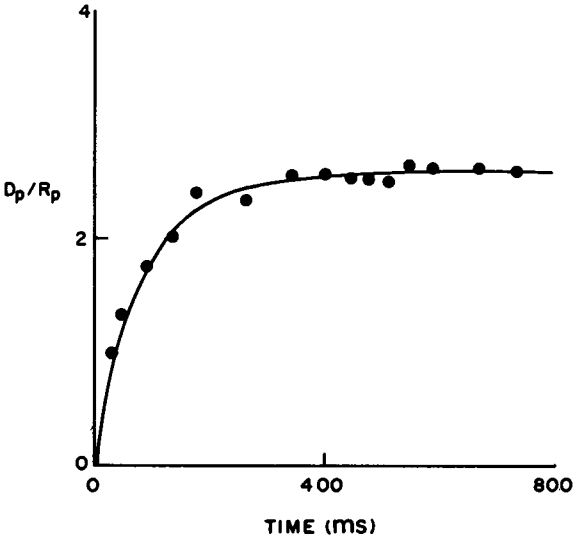

FIGURE 6 Representation of the experimental data on the creep phase as a continuous curve with two exponential terms $(D_{pm}/R_p = 2.80,\ D'_{pm}/R_p = 2.45,\ \beta_1 = 49.28,\ \beta_2 = 190.67.)$ Set No. 1. Cell No. 4923.

D_p/R_p. The theory of section 3 is then used to determine the relaxation function $G(t)$. The numerical procedure used is outlined below.

Let the interval $[0, t]$ be partitioned by n times $[t_1 = 0, t_2, \ldots, t_n = t]$. Expressing the integral in Eq. 18 as a sum of $(n-1)$ integrals and approximating each of these by the trapezoidal rule, one obtains

$$h(t_n)G_nF[A(t_n)] = F(A_p) - 2(\tau + \tau_f)\dot{A}(t_n) + \left(\frac{1}{2}\right)\sum_{k=1}^{n-1}(G_{k+1} - G_k)\{F[A(t_n) - A(t_n - t_k) + 1] + F[A(t_n) - A(t_n - t_{k+1}) + 1]\}. \quad (26)$$

Because initial conditions at $t = 0^+$ cannot be determined accurately from the experiments, the values chosen for $(\tau + \tau_f)$ and $G^*(0)$ are somewhat arbitrary. However it may be shown that the uncertainty does not have much effect on $G^*(t)$.

By fitting the experimental data with Eq. 34, the relaxation function $G^*(t)$ for a particular (D_p/R_p) was numerically calculated and plotted vs. time t (Fig. 7). The maximum dimensionless aspiration length in this case was equal to 5.67. The membrane was assumed to have instantaneous elastic reponse and the singular part of the relaxation function was set equal to zero. The time increment Δt_k was taken equal to $\Delta t_k = (0.01\ \beta_1)$ for $t < 2\beta_1$ and was increased eventually to $\Delta t_k = (0.01\ \beta_2)$ for $t > \beta_2$. The numerical accuracy was checked by running the same data with smaller time increments (dividing Δt_k by 5 and 10) that produced negligible changes in the calculated relaxation function. The assumed value of $G^*(0)$ does not affect the solution appreciably because the time increment Δt_k used is sufficiently small, i.e., $G^*(t)$ approaches the same value within a short period of time independent of the initial values.

The above numerical procedure was used to compute the relaxation function corresponding to different experiments with different D_{pm}/R_p ratios. As illustrated in Fig. 8, it is not possible to obtain a unique relaxation function for data with different maximum aspiration ratios (D_{pm}/R_p). The ratio $G^*(0)$ of the instantaneous to steady-state response increases and the integral $I_1 = \int_0^t [G^*(t) - G^*(\infty)]\,dt$ decreases with increasing D_{pm}/R_p. This shows that the nonlinearity of the stress-strain response and the time dependence are not separable.

Another approach to the calculation of the material properties would be to assume the form of the relaxation function and then to fit the (D_p/R_p) vs. time data as well as possible by adjusting this relaxation function. For example, the relaxation function for a standard solid membrane may be written as

$$G(t) = [(\gamma - 1)e^{-t/\tau_0} + 1] \quad (27)$$

where $\lambda = G^*(0)$. The (D_p/R_p) vs. time curves were obtained numerically using the relaxation function, Eq. 27, for various values of γ and (D_{pm}/R_p). It is possible to fit the rapid phase of the micropipette experiments with these curves by allowing the parameters γ and τ_0 of the relaxation function, Eq. 27, to vary as a function of the dimensionless pressure difference $(\Delta PR_p/\mu)$. It is observed that the value $[(\gamma - 1)\tau_0]$ decreases with increasing $(\Delta PR_p/\mu)$, which agrees with the results of computations of the relaxation functions described earlier in this section. To develop a better understanding of this behavior of the

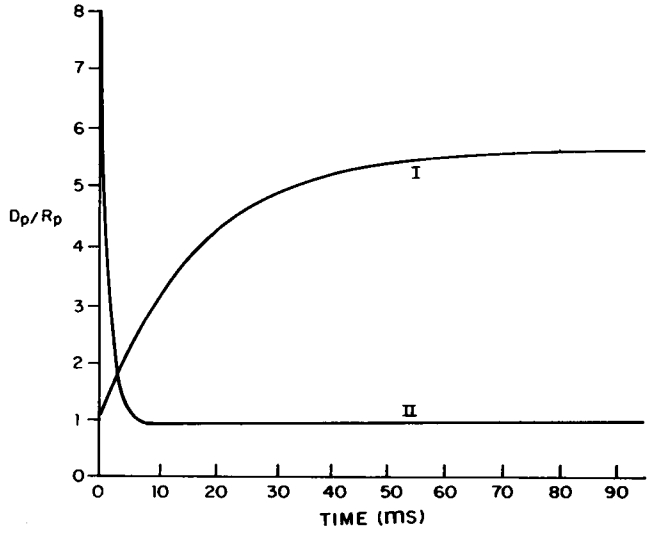

FIGURE 7 Computation of the relaxation function for a given aspiration length history. I, aspiration history curve (D_p/R_p); II, relaxation function G, $(D_{pm}/R_p) = 5.67$.

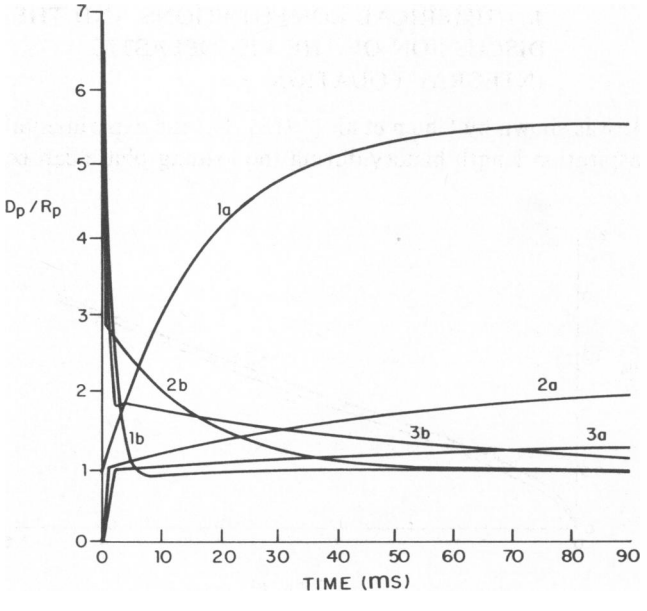

FIGURE 8 Comparison of relaxation functions computed for different values of dimensionless step pressure $(\Delta PR_p/\mu)$ as a function of time t. (*a*) D_p/R_p vs. time; (*b*) corresponding relaxation function G. D_{pm}/R_p is 5.67 (*1*), 3.62 (*2*), and 1.61 (*3*).

experimental data, the rate of strain $\dot{V}_{11} = (\dot{D}_p/R_p)$ at the tip of the pipette was computed at various stages of deformation for several sets of experimental data. In this case, a measure of deformation X_D is introduced

$$X_D = \frac{D_{pm}}{R_p} - \frac{D_p}{R_p}. \tag{28}$$

Next, $(\dot{D}_p/R_p)$ is expressed as a function of X_D. It was observed that $(\dot{D}_p/R_p)$ did not explicitly depend on (D_{pm}/R_p) but varied almost linearly as a function of X_D in the range of computations, $1 < (D_{pm}/R_p) < 7$. The functional dependence of $(\dot{D}_p/R_p)$ on X_D is obtained from the experimental data by fitting the data first with Eq. 34 and then taking its derivative. Results are shown in Fig. 9 for various experimental loading curves. If the cell membrane behaved as a Kelvin body or a standard solid, all curves in Fig. 9 would coincide. However, experimental data clearly show the nonlinear behavior of the cell membrane. The strain rate $(\dot{D}_p/R_p)$ depends not only on X_D but also on (D_{pm}/R_p). A relaxation function that is a function of deformation history is needed to explain the behavior of these experimental data.

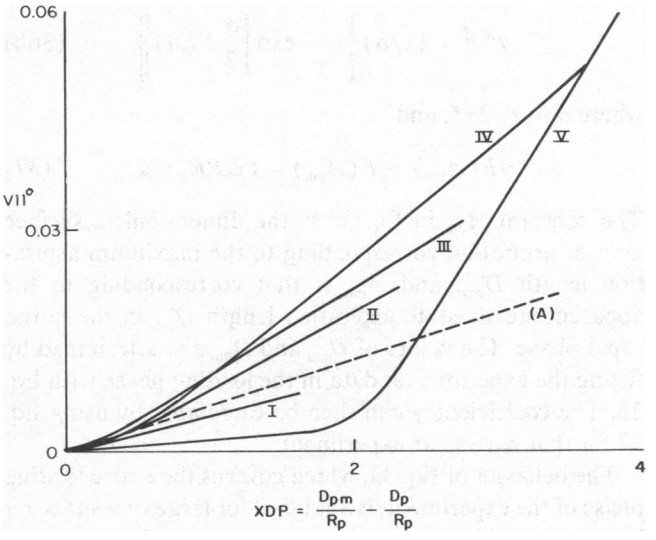

FIGURE 9 Rate of strain $V_{11} = V_{11}^0$ at the tip of the pipette obtained by fitting various experimental data as a function of the measure of expected deformation $X_p = (D_{pm}/R_p) - (D_p/R_p)$. *A*, Kelvin membrane ($\tau$ = 100 ms). The D_{pm}/D_p is 1.64 for I, 2.35 for II, 2.80 for III (Cell No. 4923), 3.60 for IV (Cell No. 4929), 5.67 for V.

5. RELAXATION FUNCTION WITH SHEAR-THINNING BEHAVIOR

Because the experimental data cannot be fitted by a model with constant properties, a nonlinear model with shear thinning is developed in this section. The relaxation function describing the behavior of erythrocyte membranes during the loading phase will be assumed to be of the form

$$G(t, I_1, \dot{I}_1) = \mu[\gamma\tau_1(I_1, \dot{I}_1)\delta(t) + (\gamma - 1)e^{-t/\tau_2} + 1] \tag{29}$$

where I_1 is the strain invariant defined by Eq. 3. The long time constant observed in experimental curves is incorporated into the relaxation function (Eq. 29) by the exponential term with time constant τ_2. The steady-state elasticity coefficient μ was determined by previous studies as $\mu = (\Delta P R_p)/F(A_p)$.

The shear-thinning behavior may be conveniently incorporated by assuming the time constant τ_1 to depend on I_1. The time constant τ_1 is assumed to decrease with increasing strain rate:

$$\tau_1 = \tau^*/(1 + \tau'\dot{I}_1/\{2[I_1(I_1 + 4)]^{1/2}\}) \tag{30}$$

where τ^* and τ' are constants. The stretch ratio λ_1 and its material derivative $\dot{\lambda}_1$ can be expressed in terms of I_1 and $\dot{I}_1$ as follows:

$$\lambda_1^2 = \{(I_1 + 2) + [I_1(I_1 + 4)]^{1/2}\}/2, \tag{31}$$

$$\dot{\lambda}_1/\lambda_1 = \dot{I}_1/\{2[I_1(I_1 + 4)]^{1/2}\}. \tag{32}$$

The analysis developed in section 3 permits the governing equation corresponding to the relaxation function, Eq. 23, for the entire loading phase to be written as

$$F(A_p) = \frac{2\gamma\tau^*}{\tau'}\ln\left[1 + \frac{\tau'}{2}\dot{A}\right] + [(\gamma - 1)e^{-t/\tau_2} + 1]F[A(t)] + \frac{(\gamma - 1)}{\tau_2}\int_0^t e^{-(t-s)/\tau_2} F[A(t) - A(s) + 1]\,ds. \tag{33}$$

The integral equation (33) may be solved numerically by the finite difference scheme presented in section 4. The solution is costly if high accuracy is demanded for large t. However, the behavior of Eq. 33 may be studied for the rapid phase of deformation by approximating the relaxation function (Eq. 29) with the simpler relation

$$G(t, I_1, \dot{I}_1) = \gamma\mu[\tau_1\delta(t) + 1] \tag{34}$$

where τ_1 is given by Eq. 32. By the use of Eq. 10, the deviatoric stress $(T_1 - T_2)$ can be expressed in this case as

$$T_1 - T_2 = \gamma\mu[(\lambda_1^2 - \lambda_1^{-2}) + 4\tau_1\dot{\lambda}_1/\lambda_1]. \tag{35}$$

The time-dependent deformation and the subsequent relaxation inside the pipette can be calculated by combining Eqs. 32 and 35 and then substituting the result into the equilibrium equation (17):

$$\tau^*\dot{A} = (1/\alpha)\left(\exp\left\{\frac{\alpha}{2}[F(A'_{pm}) - F(A)]\right\} - 1\right) \tag{36a}$$

$$\tau^* \dot{A} = (1/\alpha)\left\{1 - \exp\left[\frac{\alpha}{2} F(A)\right]\right\} \qquad (36b)$$

where $\alpha = \tau'/2\tau^*$, and

$$\gamma F(A'_{pm}) = F(A_{pm}) = (\Delta P R_p)/\mu. \qquad (37)$$

The constant A_{pm} in Eq. 37 is the dimensionless surface area of aspiration corresponding to the maximum aspiration length D_{pm}, and A'_{pm} is that corresponding to the apparent steady-state aspiration length D'_{pm} in the initial rapid phase. The values of D_{pm} and D'_{pm} are determined by fitting the experimental data in the loading phase with Eq. 25. The coefficient γ can then be calculated by using Eq. 37 for that particular experiment.

The behavior of Eq. 33, which governs the entire loading phase of the experiment, is analyzed for large times ($t > \tau_2$) by assuming that ($\gamma - 1$) is a small number and that $\tau_1 \ll \tau_2$. In that case, the integrand appearing in Eq. 33 can be shown to satisfy the following relation for $t > \tau_2$ and $\tau^* < s < t$:

$$\begin{aligned} F[A(t) - A(s) + 1] &\simeq |A(t) - A(s)| \\ &< |A_{pm} - A'_{pm}| < F[(A_{pm}) - F(A'_{pm})] \\ &= (\gamma - 1) F(A_{pm}). \end{aligned} \qquad (38)$$

It is then apparent that the contribution of the integral term to the right hand side of Eq. 33 is on the order of $(\gamma - 1)^2$. The retention of terms of order $(\gamma - 1)$ in Eq. 33 gives a simpler relation:

$$F(A_p) = \gamma \tau^* \dot{A} + [(\gamma - 1) e^{-t/\tau_2} + 1] F[A(t)]. \qquad (39)$$

Furthermore if (τ^*/τ_2) is assumed to be of order $(\gamma - 1)^2$, one obtains a simple equation for $F(A)$:

$$F(A) \simeq F(A_p)\,[1 - (\gamma - 1)\, e^{-t/\tau_2}]. \qquad (40)$$

Eq. 40 shows that the time constant τ_2, which appears in the relaxation function of Eq. 29, is approximately equal to the time constant β_2, Eq. 25, which is used to fit the data.

The above simplified relations were used to obtain the values of μ, γ and τ_2 from data on the loading phase of the micropipette experiments. The mean value of μ was estimated as 4.2×10^{-3} dyn/cm by Chien et al. (1980). The average value of γ estimated from data of Chien et al. (1978) is $\gamma = 1.25 \pm 0.20$. The time constant τ_2 in the relaxation function (29) is assumed to be equal to the time constant $\beta_2 = 5.04 \pm 3.12$ s. of the slow deformation phase. The order of magnitude of τ^* is also known. The time constant of the rapid phase of deformation reported by Chien et al. (1978) approaches the value of τ^* as $V_{11} \to 0$. This is the limiting case of experiments conducted with small pressure differences [$1.0 < (D_{pm}/R_p)$ (1.5)] across the pipette. Using the results of Chien et al. (1978) the value of τ^* in the present investigation is estimated as $\tau^* = 100$ ms.

The shear-thinning behavior of the membrane with a relaxation function (Eq. 29) depends strongly on the value of α which is defined as the ratio of two time constants ($\alpha = \tau_1/2\tau^*$). To choose the appropriate value of α the loading curve obtained by solving Eq. 36 is compared with the corresponding curve of the Kelvin material membrane. For fixed (D_{pm}/R_p), the experimental data may be fitted by a Kelvin model with time constant τ_{D1}. The constant α is then adjusted to match the Kelvin model in the initial stages of the rapid phase of deformation. This constant value of α yields a model which resembles a Kelvin model, but with a variable time constant τ'_{D1} depending on (D_{pm}/R_p). The time constant τ_{D1} observed in experimental data (Fig. 14 of Chien et al. [1978]) is compared in Fig. 10 with τ'_{D1} of the shear-thinning membrane for fixed α and various (D_{pm}/R_p) values. From this graph it may be concluded that $\alpha \simeq 0.5$ and $\tau^* = 100$ ms give adequate results matching the experimental observation in the range [$1.5 < (D_{pm}/R_p) < 5.01$]. Fig. 11 shows a comparison of the initial phase of several experimental deformation curves with the corresponding curves of the shear-thinning material obtained by solving Eq. 36a. The above procedure leads to good agreement with the experimental data.

The time constant τ_1 computed by the above procedure is actually the summation of the time constant of the membrane and another term, τ_f, which is introduced by Eq. 16 to account for fluid dissipation inside and outside the cell. However, it was illustrated by Chien et al. (1978) that fluid dissipation in their experiments was small compared to the dissipation in the membrane.

6. DISCUSSIONS AND CONCLUSIONS

In the present investigation the results of Chien et al. (1978) obtained from the data on the loading phase of the

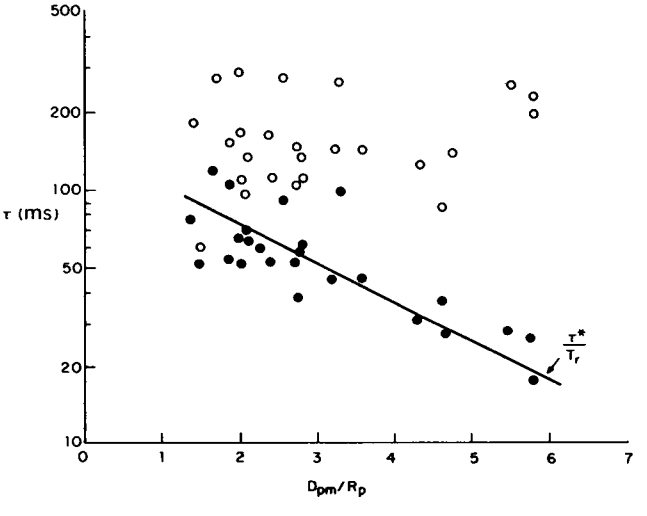

FIGURE 10 Variation of the time constant of the rapid phase of deformation (τ_{D1}) with the degree of deformation (D_{pm}/R_p). The data is matched by the theoretical predictions τ'_{D1} of the shear-thinning material for $\alpha = 0.5$.

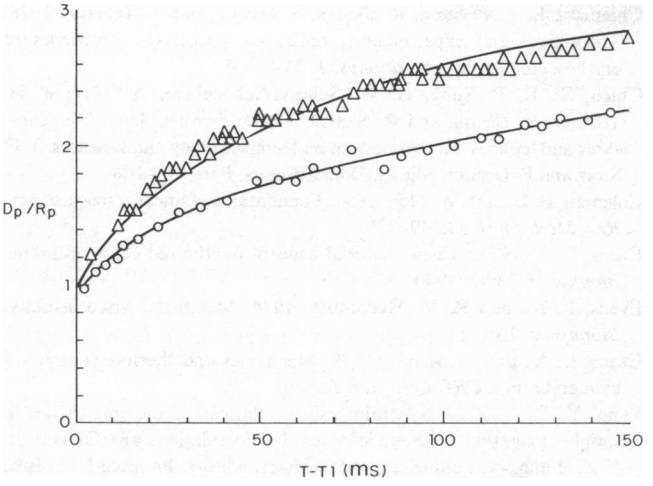

FIGURE 11 Experimental aspiration length history obtained for two erythrocytes subjected to different degrees of deformation plotted against time. The data points are matched by theoretical curves (solid lines) obtained by solving Eq. 47a. O, Cell No. 4923, $D_{pm}/R_p = 2.80$, $\tau^* = 100$ ms. Δ, Cell No. 4929, $D_{pm}/R_p = 3.60$, $\tau^* = 100$ ms.

micropipette experiment have been modeled by using a viscoelastic constitutive equation in the form of a single integral relation. It is proposed that the viscoelastic properties of erythrocyte membrane under continuous deformation (stress) can be described by the integral relation (Eq. 8) with a relaxation function (Eq. 40). This relaxation function incorporates the shear-thinning behavior observed in the micropipette experiments. The formulation given in section 2 may be useful to describe the deformations of other biological membranes.

The single integral constitutive equations of the present investigation can be considered as the first term of the integral series representation given by Pipkin and Rogers (1968) to describe nonlinear viscoelastic response to an arbitrary strain (stress) history. As reported by Pipkin and Rogers (1968), experimental evidence suggests that the most severe trial of the extrapolation from one-step data is not its ability to predict closely the results for smooth histories, but its accuracy in forecasting the results of two-step tests, particularly creep and recovery tests. The second term of the series is determined directly and completely by the discrepancy between two-step data and the extrapolation from one-step data. The recovery phase of the micropipette experiments may be regarded as a second (negative) step of applied pressure that forms a severe test of the efficacy of the single integral approach.

Numerical results obtained from the recovery phase of the micropipette experiment by using the approximate relaxation function (Eq. 45) show that the time constant τ_R of the relaxation phase is nearly equal to the time constant τ_{D1} of the rapid deformation of the loading phase (with the same shear-thinning property) for relaxation taking place after short periods of deformation. However, experimental results presented by Chien et al. (1978) show that after long periods of deformation ($t > 20$ s) the relaxation time constant τ_R does not show a dependence on the degree of deformation and its value is nearly equal to τ^*. This type of behavior cannot be explained by single integral relationships. Such theories would predict that the recovery after a long term deformation is as fast as the initial loading phase. Hence the recovery of cell membranes after long periods of deformation cannot be represented by the viscoelastic constitutive equation of the present investigation. It is suggested by Chien et al. (1978, 1980) that the material properties undergo dynamic changes depending on the extent and duration of deformation as a result of molecular arrangement in response to a fixed membrane strain. The present investigation supports this premise.

A factor which has not been taken into account in the present analysis but may have some influence at large aspiration lengths is the possibility of buckling of the erythrocyte membrane at the tip of the pipette. The compression in the circumferential direction at the tip of the pipette may be fairly large and it may be energetically favorable for the membrane to buckle or wrinkle in this vicinity. At the resolution of the light microscope in which the experimental results used here were made, a minor degree of buckling would not be visible. The influence of buckling would be to reduce the stress in the circumferential direction. There will then result a concomitant reduction of the stress in the axial direction in the membrane. Hence such buckling could be responsible for some part of the shear-thinning behavior observed.

7. APPENDIX

Analysis of Axisymmetric Deformation of Membranes

The equations governing large axisymmetrical deformations of nonlinear elastic membranes are discussed by Green and Adkins (1960). The equations can be reduced to a system of ordinary differential equations which may be integrated numerically. A convenient reformulation is given by Yang and Feng (1970) in terms of three first-order ordinary differential equations with explicit derivatives.

For membranes of constant surface area, only two dependent variables are needed to describe axisymmetric deformations. These could be the dimensionless coordinates R, Z (defined at the beginning of section 3) as functions of dimensionless initial radius $R_0 = R_0'/R_p$. Here, R and R_2 (where $R_2 = R/\sin\theta$) will be chosen as dependent variables, retaining R_0 as the independent variable. The angle θ is the inclination of a normal to the membrane relative to the axial direction; R_2 is the radius of curvature in the circumferential direction.

The relation of R to R_0 can be expressed as an ordinary differential equation by using the constant area stipulation:

$$(dR/dR_0) = (R_0/R)\,(dS_0/dR_0)\,(R_2^2 - R^2)^{1/2}/R_2 \quad (A1)$$

where $S_0 = S_0'/R_p$ and S_0' is the arc length along the undeformed meridian.

The differential equation for R_2 is obtained by combining the equilibrium equations along the meridian of the deformed surface and along the axis of the pipette. The result is

$$(dR_2/dR_0) = 2(dR/dR_0)(\mu/\Delta PR_p)\,(T_2 - T_1)/\mu R). \quad (A2)$$

In the case of Evans's constitutive equation (4), Eq. A2 reduces to

$$(dR_2/dR_0) = 2(\mu/\Delta PR_p)(dR/dR_0)\left[\frac{-R_0^2}{R^3} + \frac{R}{R_0^2}\right]. \quad (A3)$$

Eqs. A1 and A2 constitute a system of first-order differential equations that can be integrated numerically by the Runge-Kutta method. The boundary conditions for the cap in the micropipette are

$$\begin{aligned} R &= 0 \\ R_2 &= R_k \end{aligned} \qquad \text{at } R_0 = 0, \quad (A4)$$

where R_k is a constant that must be determined in the process of solution. The last term on the right hand side of (A3) becomes indeterminate at the pole $R = R_0 = 0$. To calculate its proper limit, let

$$Z = (R^2/2R_k) + 0(R^4) \text{ for } R < \epsilon \quad (A5)$$

where ϵ is small. Using the constant area requirement Eq. A3 then reduces to

$$(dR_2/dR_0) = -(4/R_k)\,(\mu/\Delta PR_p)\,R, R < E. \quad (A6)$$

Eq. A6 is used instead of A3 to begin the numerical integration procedure.

The axial distance from the pole, and the surface area of the cap may be obtained by using the additional differential equations

$$(dZ/dR_0) = R_0/R_2, (dA/dR_0) = 2R_0. \quad (A7)$$

The above system is integrated to give the results shown in Figs. 5 and 6.

The authors would like to thank Mr. Charles Chan for his competent help with the numerical computations. This investigation was supported by National Heart, Lung, and Blood Institute grant HL 16851 and North Atlantic Treaty Organization Travel and Research grant 110-80.

Received for publication 8 May 1981 and in revised form 23 December 1981.

REFERENCES

Chien, S. 1975. Biophysical behavior of red cells in suspensions. *In* The Red Blood Cells. D. Mac N. Surgenor, editor. Academic Press, Inc., New York. 2nd edition. 2:1031–1133.

Chien, S., K.-L. P. Sung, R. Skalak, S. Usami, and A. Tözeren. 1978. Theoretical and experimental studies on viscoelastic properties of erythrocyte membrane. *Biophys. J.* 24:463–487.

Chien, S., K. P. Sung, G. W. Schmid-Schoenbein, A. Tözeren, H. Tözeren, S. Usami, and R. Skalak. 1980. Microrheology of erythrocytes and leukocytes. Symposium on Hemorheology and Diseases. J. F. Stolz and P. Drouin, editors. Doin Editeurs, Paris. 93–108.

Coleman, B. D., and W. Noll. 1961. Foundations of linear viscoelasticity. *Rev. Mod. Phys.* 33:249–299.

Evans, E. A. 1973. A new material concept for the red cell membrane. *Biophys. J.* 13:926–940.

Evans, E. A., and R. M. Hochmuth. 1976. Membrane viscoelasticity. *Biophys. J.* 16:1–11.

Evans, E. A., and R. Skalak. 1979. Mechanics and thermodynamics of biomembranes. *CRC Crit. Rev. Bioeng.*

Fung, Y. C. 1972. Stress-strain history relations of the soft tissues in simple elongation. *In* Biomechanics: Its Foundations and Objectives. Y. C. Fung, N. Perone, and M. Anliker, editors. Prentice-Hall, Inc., Englewood, NJ. 181–208.

Green, A. E., and Adkins, J. E. 1960. Large Elastic Deformations. Clarendon Press, Oxford. 133–171.

Lee, E. H., and T. G. Rogers. 1963. Solution of viscoelastic stress analysis problems using measured creep of relaxation functions. *J. Appl. Mech.* 128–133.

Pipkin, A. C., and T. G. Rogers. 1968. A non-linear integral representation for viscoelastic behavior. *J. Mech. Phys. Solids.* 16:59–72.

Schmid-Schöenbein, H. 1976. Microrheology of erythrocytes, blood viscosity and the distribution of blood flow in the microcirculation. *In* International Review of Physiology and Cardiovascular Physiology. A. C. Guyton and A. W. Cowley, editors. University Park Press, Baltimore. 9, part 2:1–62.

Skalak, R., A. Tözeren, R. P. Zarda, and S. Chien. 1973. Strain energy function of red blood cell membranes. *Biophys. J.* 13:245–264.

Skalak, R. 1976. Rheology of the red blood cell membrane. *In* Microcirculation. J. Grayson and W. Zingg, editors. Plenum Publishing Corp., New York. 1:53–70.

Wineman, A. S. 1972. Large axially symmetric stretching of a nonlinear viscoelastic membrane. *Int. J. Solids Structures.* 8:775–790.

Wineman, A. S. 1978. Bifurcation of response of a nonlinear viscoelastic spherical membrane. *Int. J. Solids Structures.* 14:197–212.

Yang, W. H. and W. W. Feng. 1970. On axisymmetrical deformations of nonlinear membranes. *J. Appl. Mech.* 37:1002–1011.